INL/EXT-16-39932

Light Water Reactor Sustainability Program

Study of the Effect of Swelling on Irradiation-Assisted Stress Corrosion Cracking

September 2016

U.S. Department of Energy

Office of Nuclear Energy

INL/EXT-16-39932

Study of the Effect of Swelling on Irradiation-Assisted Stress Corrosion Cracking

S. Teysseyre

September 2016

Prepared for the
U.S. Department of Energy
Office of Nuclear Energy

ABSTRACT

This report describes the methodology used to study the effect of swelling on the crack growth rate of an irradiation-assisted stress corrosion crack that is propagating in highly irradiated stainless steel 304 material irradiated to 33 dpa in the Experimental Breeder Reactor-II. The material selection, specimens design, experimental apparatus and processes are described. The results of the current test are presented.

CONTENTS

FIGURES

TABLES

ACRONYMS

AISI	American Iron and Steel Institute
CGR	crack growth rate
CT	compact tension
IASCC	irradiation-assisted stress corrosion cracking

Study of the Effect of Swelling on Irradiation-Assisted Stress Corrosion Cracking

1. INTRODUCTION

To predict the susceptibility of high-fluence materials to irradiation-assisted stress corrosion cracking (IASCC), it is necessary to estimate how the features appearing at high fluence may affect IASCC. One of those features is void swelling. In a material with a voided microstructure, one can expect the high density of voids (both intergranular and intragranular) to affect the propagation of a stress corrosion crack. An intragranular void may affect local stress and deformation and the presence of intergranular voids and bubbles may affect grain boundary cohesion and any diffusion process on the grain boundary. To study the effect of void swelling on IASCC crack propagation, this project is testing a highly irradiated material whose irradiation conditions generate a swelling gradient through the component. This report describes the material selected, the methodology and procedures put in place for the study, and the initial results of the first completed test.

2. MATERIAL HISTORY

The material was cut from a thick hexagonal block made of American Iron and Steel Institute (AISI) 304 stainless steel that served in one of the reflector assemblies in the Experimental Breeder Reactor-II fast reactor. The chemical composition is Fe-19.26Cr-8.81Ni-1.57Mn-0.43Si-0.056C-0.027P-0.03S wt%. The material was not fully annealed before irradiation, as indicated by microstructure characterization of archive material suggests 5% cold work at the center of the block. The doses received and irradiation temperatures are evaluated from the temperature and dose calculated for the encasing duct using reactor physics and heat transfer calculation (Bond 1999, Garner 2006, Garner 2007). This block was part of a series of five blocks that were in the reactor for 13 years: 4.5 years in Row 8 and 8.5 years in Row 16. However, most of the dose received (i.e., 97%) was received in Row 8. The material comes from Block 3 that was in the center of the core and received the most dose (i.e., from 33 dpa for the face located toward the core center to about 22 dpa for the opposite face). More specifically, the material comes from a 0.5-in.-thick coin labelled 3F3 that was initially located toward the center of Block 3 (Figure 1). The time-averaged temperature was 390°C; however, due to gradient gamma heating, there was an off-center peak in temperature inside the block (Figure 2). The maximum average temperature inside Block 3 is estimated to be about 460°C (Garner 2014). This temperature gradient is expected to have led to a swelling gradient. Ultrasonic time-of-flight measurements performed on Coin 3F3 confirmed an off-center swelling peak, with a maximum at about 3.7% swelling and a minimum less than 2% (Garner 2013, Garner 2014).

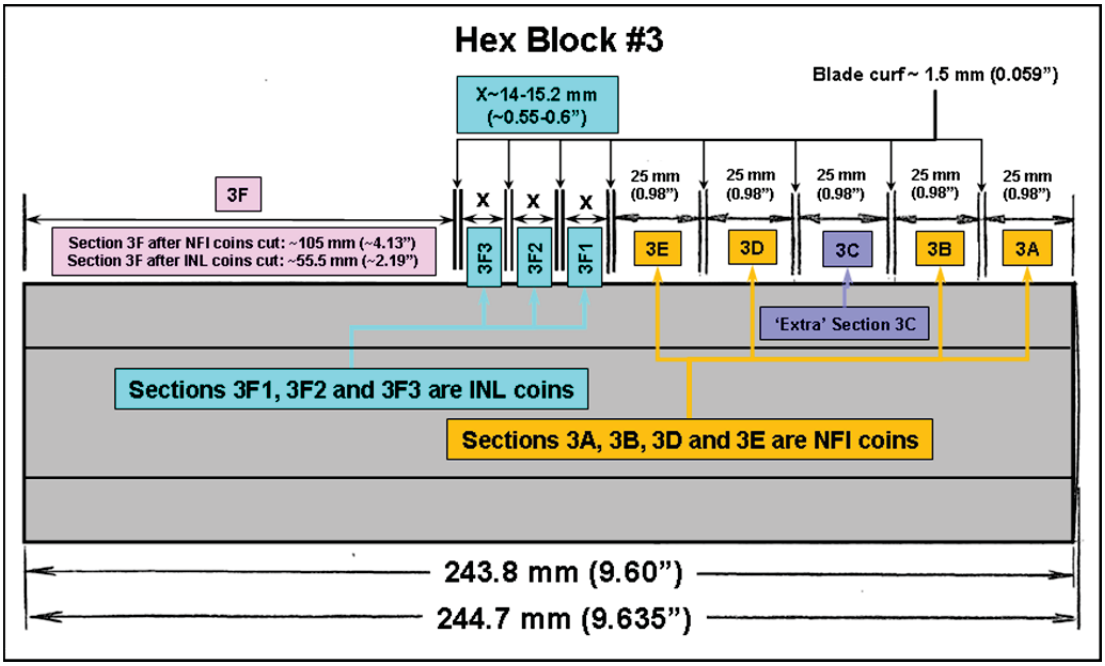

Figure 1. Schematic of Block 3 from which the material used for this study (Coin 3F3) was cut.

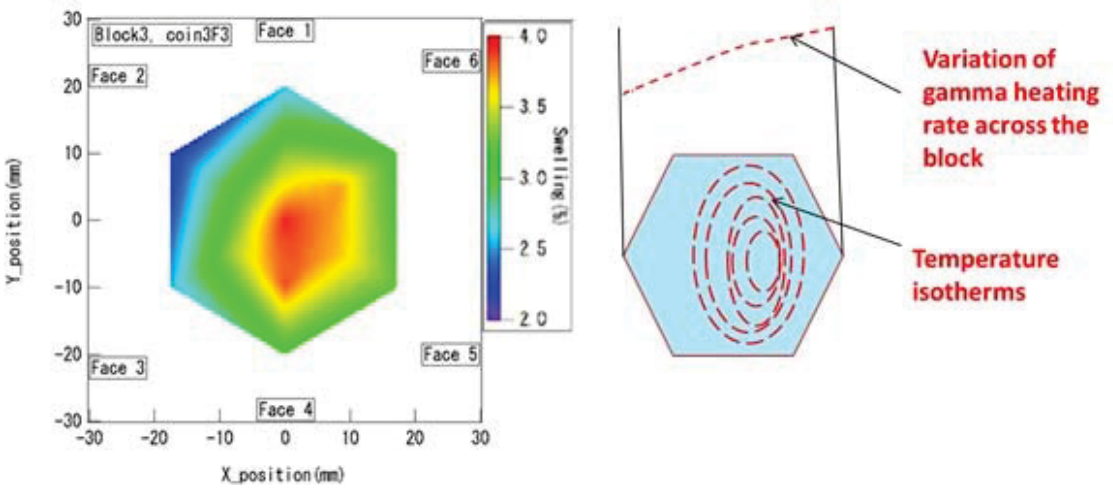

Figure 2. Temperature distribution across the block (Garner 2014).

3. SPECIMEN MACHINING

Two pairs of compact tension (0.25T CT) specimens were machined. The location for machining was determined such as, for each pair of CT specimens, the cracks will grow in a material with similar swelling. Two specimens were machined so the cracks will grow in a material with 3.7% swelling and two specimens were machined so cracks will grow in less than 2% swelling. The percent swelling used is an estimation that is determined by ultrasonic technique. The orientation of the CTs with regard to the component was the same. Details on the machining steps can be found in INL/EXT-15-35594. The first specimens to be tested are specimens CT1 and CT2. Their location in the coin is shown in Figure 3. The specimens' dose rates are respectively 160 and 180 mR/hour at 30 cm.

For this project, it was decided that short leads will be connected to the specimens as part of the specimen machining. The small leads are placed so their connection to the direct current potential drop

leads in the autoclave will be performed without moving the specimen. A picture of the CT1 specimen with the leads attached is presented in Figure 4.

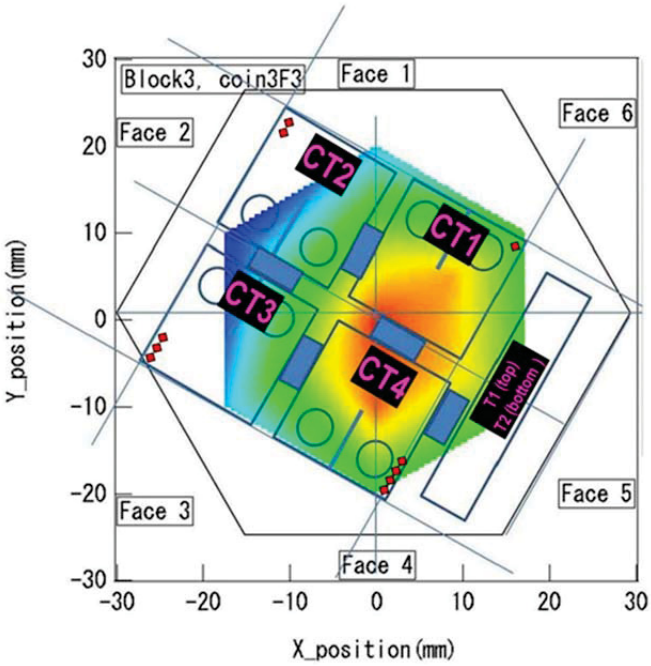

Figure 3. Location and orientation of the four CT specimens (CT1, CT2, CT3, and CT4) as they were cut in the hexagonal coin. T1 and T2 show the location of the tensile specimens.

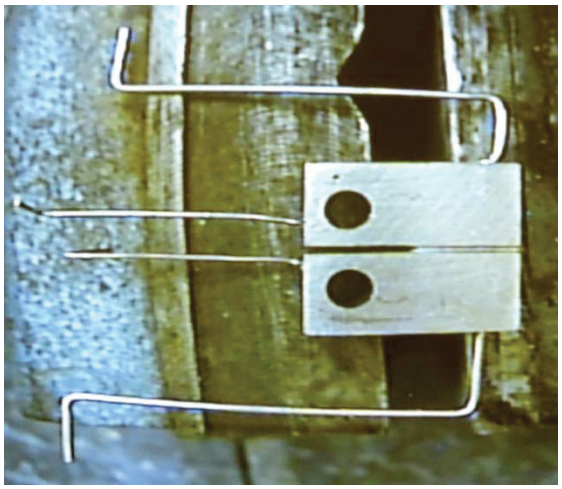

Figure 4. CT1 specimen after short current and potential lead welding is completed. Dimensions of the photograph may appear distorted because the photograph was taken from video monitor specimens.

After machining, the CT specimens were cleaned in the cell. Ultrasonic cleaning, followed by rinsing of the specimen with water, was efficient. After cleaning, no loose contamination was detected.

4. SHIPPING AND RECEPTION AT TESTING FACILITY

To minimize the number of manipulations (e.g., cask loading, unloading, and storage), it was decided the specimens would be shipped on a demand basis. Only two CT specimens were shipped to the building where testing is performed, the remaining specimens are being stored in the Westinghouse facility. Each

specimen was shipped in an individual aluminum container, maintaining the specimen in place between foam inserts, as shown in Figure 5. Each can was sealed in a plastic bag.

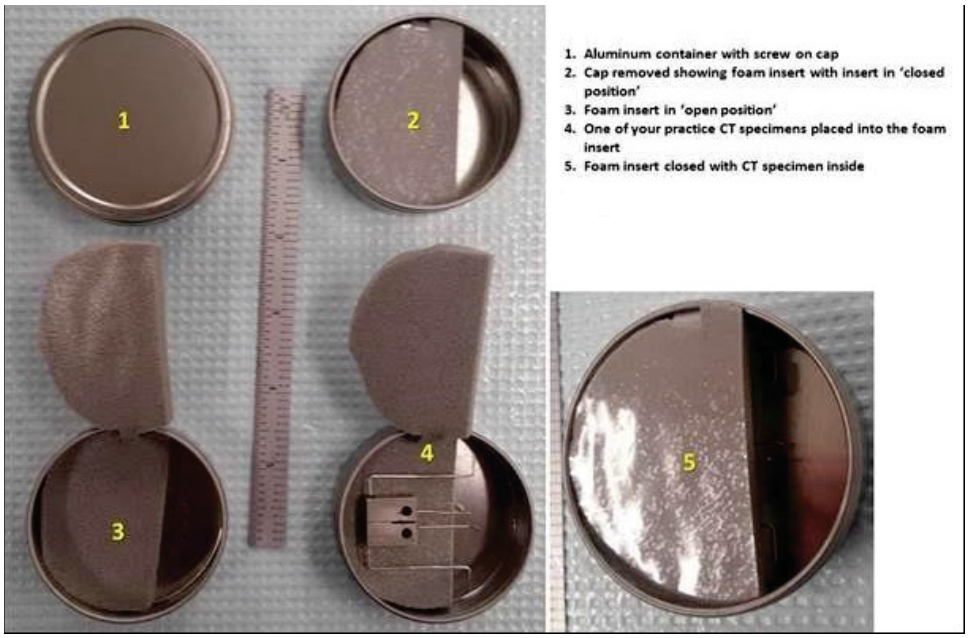

Figure 5. Packaging of CT specimens with attached leads.

After reception of the shipping cask at the facility, the plastic bags containing the specimens were transferred to a lead pig (Figure 6). This lead pig was procured for this project by the facility where the experiments are performed. It has inside dimensions of a 4-in. diameter by 12-in. high with the lid on unit and has 2-in. walls, lid, and bottom. This container is used for specimen storage and transfer to the test jig.

Figure 6. The shipping container (in blue) contains the specimens. Those specimens will be transferred to the yellow lead pig for storage and transport within the testing facility.

5. TEST FACILITY

5.1 Irradiation-Assisted Stress Corrosion Cracking Testing Facility

The IASCC test was performed in a partially shielded testing loop. Water was continuously refreshed with a flow rate of about 200 mL/minute for a 4-L autoclave; the water chemistry was continuously monitored and controlled. The dissolved gas concentration was controlled by applying an overpressure of pure hydrogen at room temperature before water flowed into the high-pressure, high-temperature part of the loop. The ion content in the water was controlled by flowing water through an ion exchanger to remove corrosion products. The test was performed in a pressurized water reactor environment, meaning pure water with 1,000 ppm of boron and 2 ppm of lithium added and 25 cc/kg of dissolved hydrogen. Water chemistry is controlled by measuring water conductivity and pH. For crack growth monitoring and load control, the AT5 software provided by the GE Global Research Center was used. Crack length was monitored using the direct current potential drop technique.

For radiation protection, a support frame was installed around the autoclave. This frame offers a work space for specimen handling. The frame safely supports enough lead to provide shielding with 4-in. of lead on the walls and 2-in. of lead plus 1-in. of steel on the floor (i.e., sample loading side). The frame is not in contact with the autoclave, which prevents heat transfer for the autoclave to the lead bricks. Each of the lead bricks being used have been powder coated to avoid any lead oxidation and any subsequent health risk hazard. A 1/8-in. steel cover protects the shield walls. The front of the cover can be lowered down to provide access to the lead bricks that comprise the front wall. The front wall can be partially removed to allow specimen loading and unloading.

5.1.1 Loading Procedure

When the specimen is brought to the facility, the laboratory space is as presented in Figure 7. The front of the shield has been partially removed to allow operator access to transfer specimens. In the autoclave, a guiding jig has been placed for precise and quick loading of the specimens into the clevises (Figure 8).

The bag containing the specimen is transferred from the yellow lead pig to the work area. The work area is equipped with a small storage niche that is available if there was a need to pause work. The can containing the specimen is removed from the plastic bag and opened. After verifying the specimen's identity, the specimen is loaded into the clevises and secured with the loading pin using long reach tongs. The guiding jig is then removed and the specimen is held in place by applying 50 lb of load.

The next step consists of welding the direct current potential drop leads to the short leads that are attached to the specimen (Figure 9). After verifying the contact is strong enough and loading is satisfactory (Figure 10), the autoclave body is lowered and the autoclave is sealed. The front shield is then put into place (Figure 11).

After loading is complete, the radiation field is measured and posted. For this specimen, the dose rate in contact with the wall of the shield is 300 μR/hour the dose rate just below the autoclave is 30 mR/hour and the dose rate just above the autoclave is 29 mR/hour). The dose rate at the boundary of the restricted area is 15 μR/hour.

5.1.2 Water Chemistry Control

During the course of the experiment, water samples were taken weekly and analyzed for contamination; water chemistry was verified using Inductively Coupled Plasma Optical emission Spectrometry (ICP-OES). The sample is acidified with Optima nitric acid to a concentration of 1%. Analysis of lithium and boron are performed on the Thermo iCAP 6500 ICP-OES. Calibration and calibration checks are National Institute of Standards and Technology traceable standards in 1% trace

metal nitric acid. A lithium two-point curve of 0 ppm lithium and 10 ppm lithium and a boron two-point curve of 0 ppm boron and 1,002 ppm boron are generated prior to sample analysis. Calibration verification is performed using a 5-ppm lithium standard and a 100-ppm boron standard. The acceptable limit for calibration verification is ±10% for each analyte. The sample is diluted with 1% trace metal nitric acid to within the calibration range if it is outside the generated calibration curve.

Figure 7. Laboratory prepared before reception of the specimen.

Figure 8. Clevises and guiding jig prepared before loading the specimen.

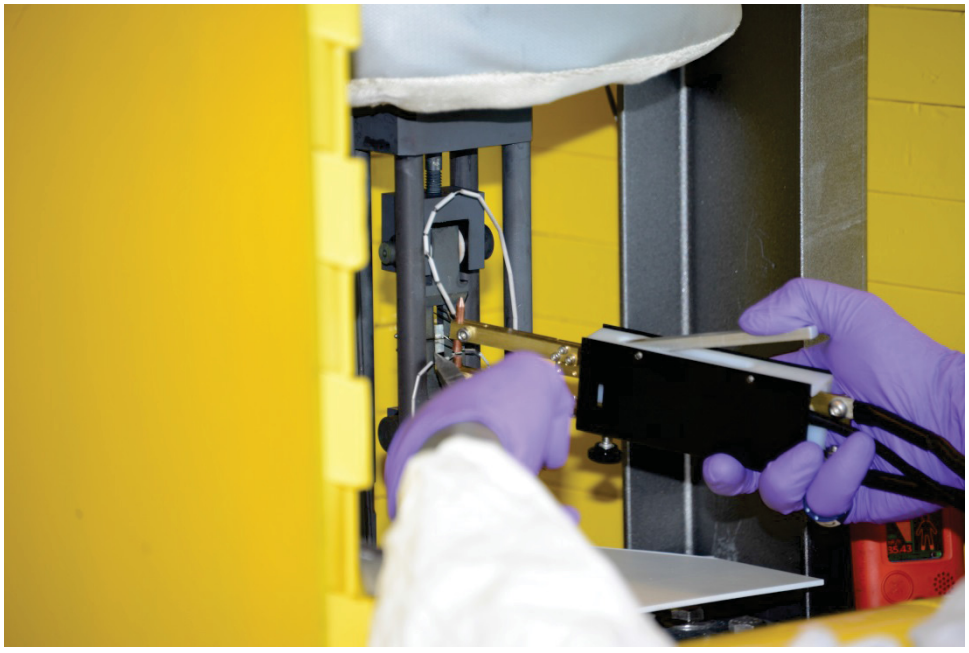

Figure 9. The direct current potential drop leads are being connected to the samples leads.

Figure 10. Specimen loaded in the autoclave and ready to be tested.

Figure 11. IASCC testing jig with shield closed.

5.2 Post Test Characterization

Traditionally, crack grown rate (CGR) experiments are ended by fatigue cracking the specimen and observation of the fracture surface. The actual measurement of the crack length is used to confirm, or correct, the CGR determined by direct current potential drop. Although this procedure may be followed, an alternative method was developed to be able to acquire additional information. Once the experiment is complete, a slice of the specimen will be retrieved and polished in order to proceed to analysis of crack propagation path, transmission electron microscopy, and atom probe tomography. The retrieved material will be used to confirm the amount of swelling in the tested specimen and to perform micromechanical tensile testing with this material. Micromechanical testing has the ability to quantify a change in cohesion of the grain boundaries. This project will characterize grain boundary cohesion of this 33-dpa 304 stainless steel with 4% and less than 2% swelling and compare the results with the determined IASCC crack growth rate of the same specimens.

5.2.1 Post Test Specimen Slicing

At completion of the CGR test, the specimen will be removed and placed in a specially designed jig (Figure 12) that is connected to a low speed saw located in a glove box. This jig will allow slicing of the specimens as described in the schematic presented in Figure 12 with minimum exposure to the operator and high repeatability. The leftover material will be cracked open for observation of the fracture surface.

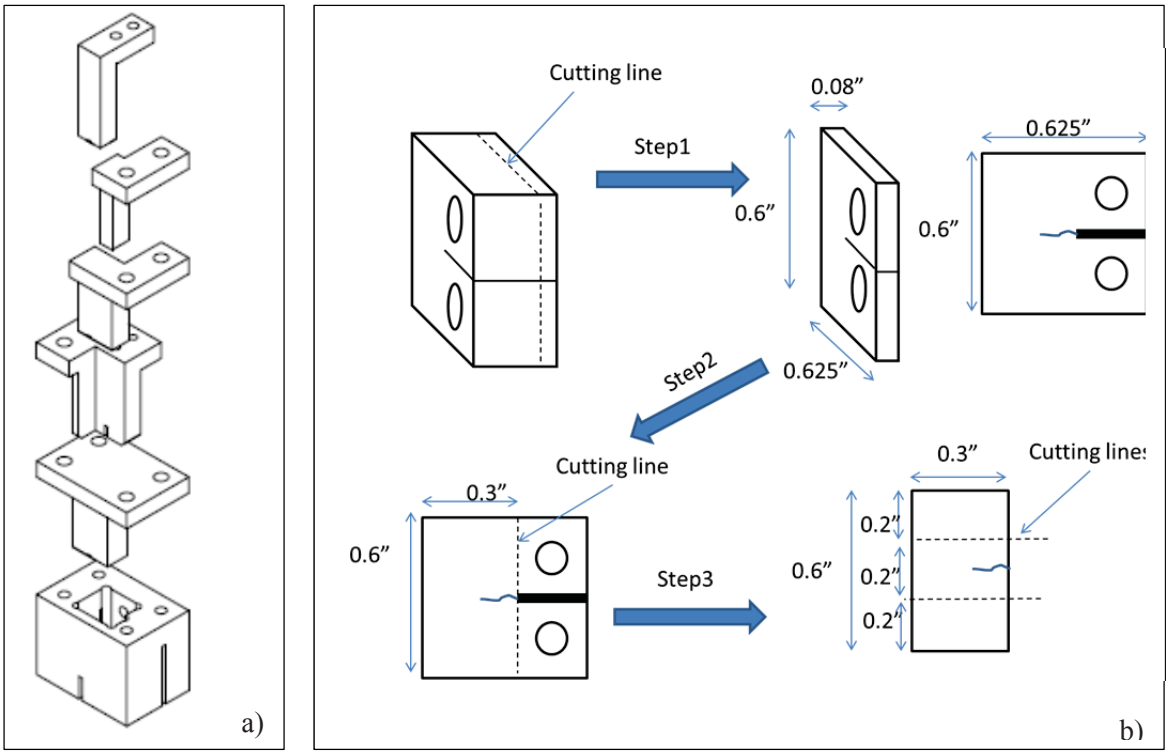

Figure 12. Schematic of the jig used to slice the 0.25T-CT specimen in the glove box (a), and the various steps taken to slice the specimen to prepare it for post test characterization.

5.2.2 Procedure for Single Grain Boundary Testing

Specimens (2 mm x 2 mm x 0.5 mm) will be extracted from the sample and shipped to the University of California-Berkeley’s Nuclear Materials Laboratory. It is anticipated that the specimens will be below this laboratory’s dose rate limit. If necessary, the specimens’ dimensions will be reduced and lift out foils will be manufactured at the Center for Advanced Energy Studies MaCs laboratory.

The grain boundaries in the samples will be located and characterized using electron backscatter diffraction. From the stock, foil micro-tensile samples will be manufactured as demonstrated by University of California-Berkeley previously (see Figure 13) under a different collaboration with Atomic Energy of Canada, Limited.

The tensile tests will be performed at room temperature as demonstrated previously.

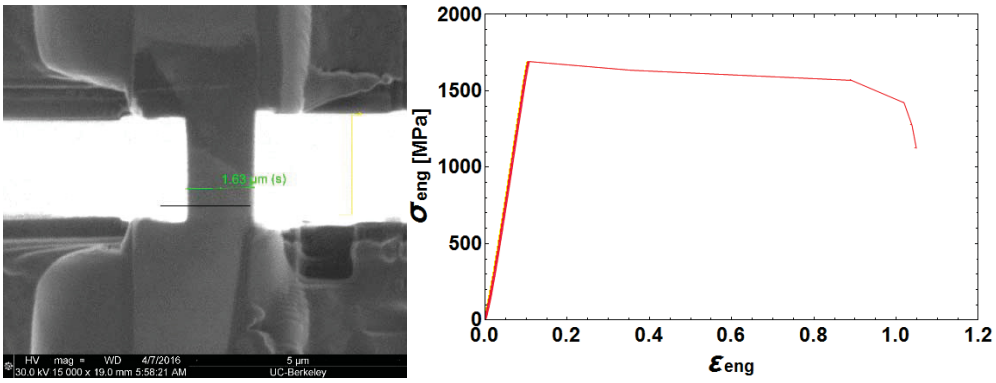

Figure 13. Tensile test geometry on lifted out samples with a grain boundary in the sample (a). Stress strain curve of the tested sample (b). Failure of the grain boundary without plastic deformation is obvious.

6. RESULTS

The specimen (ID: CT2) is a 0.25T CT specimen. The specimen is tested at a nominal applied K level of 16 ksi√in in a pressurized water reactor environment (325°C, 1,000 ppm boron, 2 ppm lithium, 25 cc/kg dissolved hydrogen). After several days in the environment to assure stabilization of the corrosion potential, the specimen was fatigue-pre-cracked at a maximum applied K of 14 ksi√in and a loading ratio of 0.3 at a frequency of 0.5 Hz. In the following pre-cracking steps, the applied K was increased to the target test K (16 ksi√in) as R was increased and holding time under load was applied. A summary of the various steps used is described in Table 1. The specimen responded well to each loading change with a nice stable crack propagation rate at each step (Figure 11). At about 630 hours, a long power outage caused a controlled interruption of the experiment. The experiment was restarted and several steps were introduced in order to verify the specimen was still responding to the solicitation. Loading was then transitioned to constant K (Figure 12).

The crack growth rate measured at constant K=16 ksi√in is 1.9×10^{-9} mm/s (or 1.9×10^{-12} m/s). From the information collected from NUREG/CR-7027, the CGR measured is about one order of magnitude below most of the data and the NUREG-0313 curve (which is about 1×10^{-10} m/s at K = 16 ksi√in). The Applied K was then increased to 18 ksi√in. under this condition, the CGR stabilized at 4.6×10^{-9} mm/s (Figure 16).

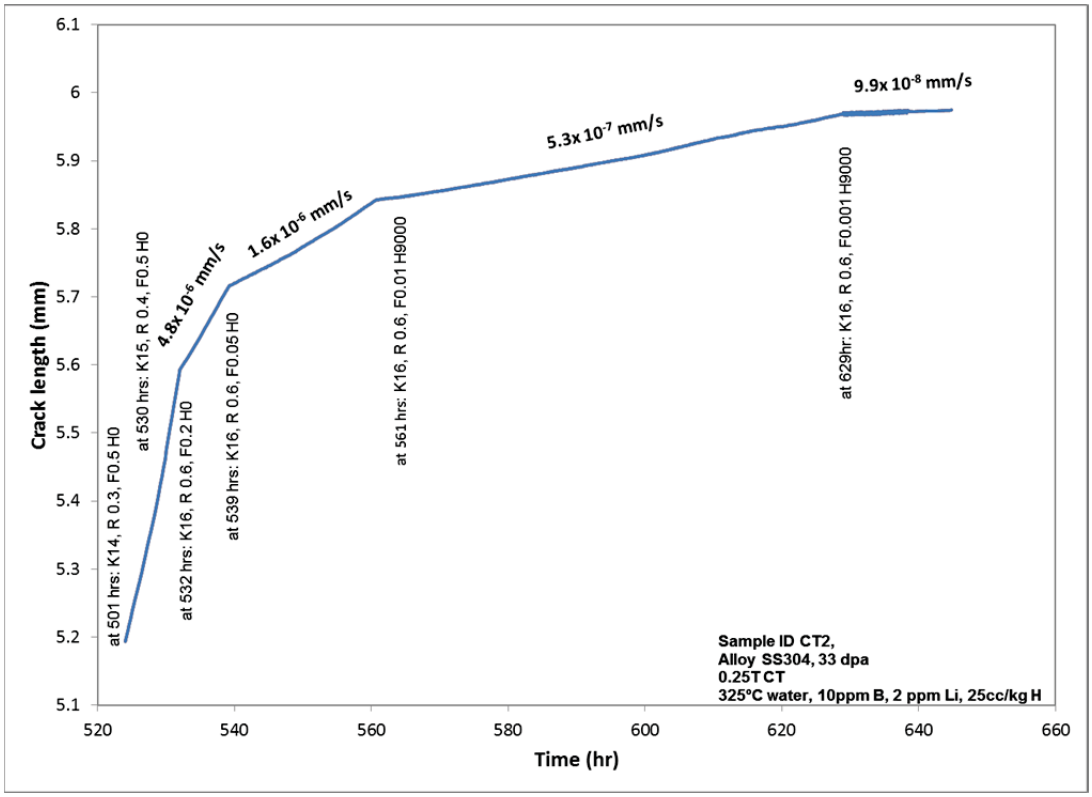

Figure 14. Initiation of the experiment, fatigue pre-crack.

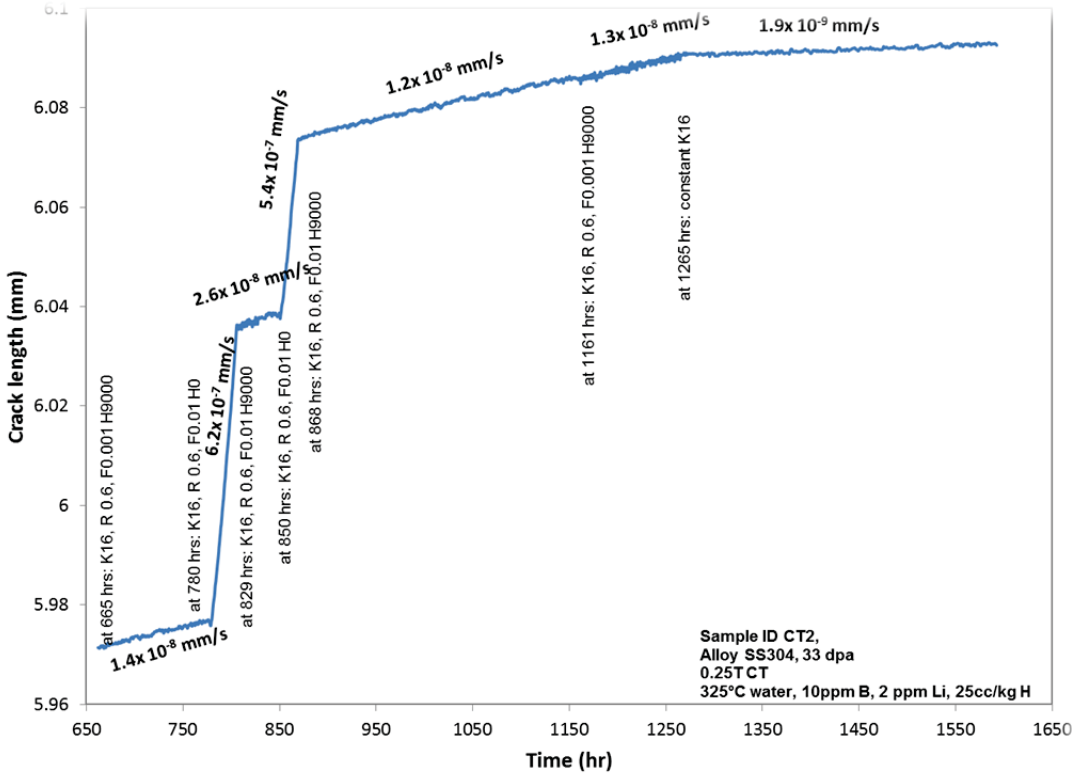

Figure 15. Second part of the experiment after restart, pre-cracking, and transition to constant K.

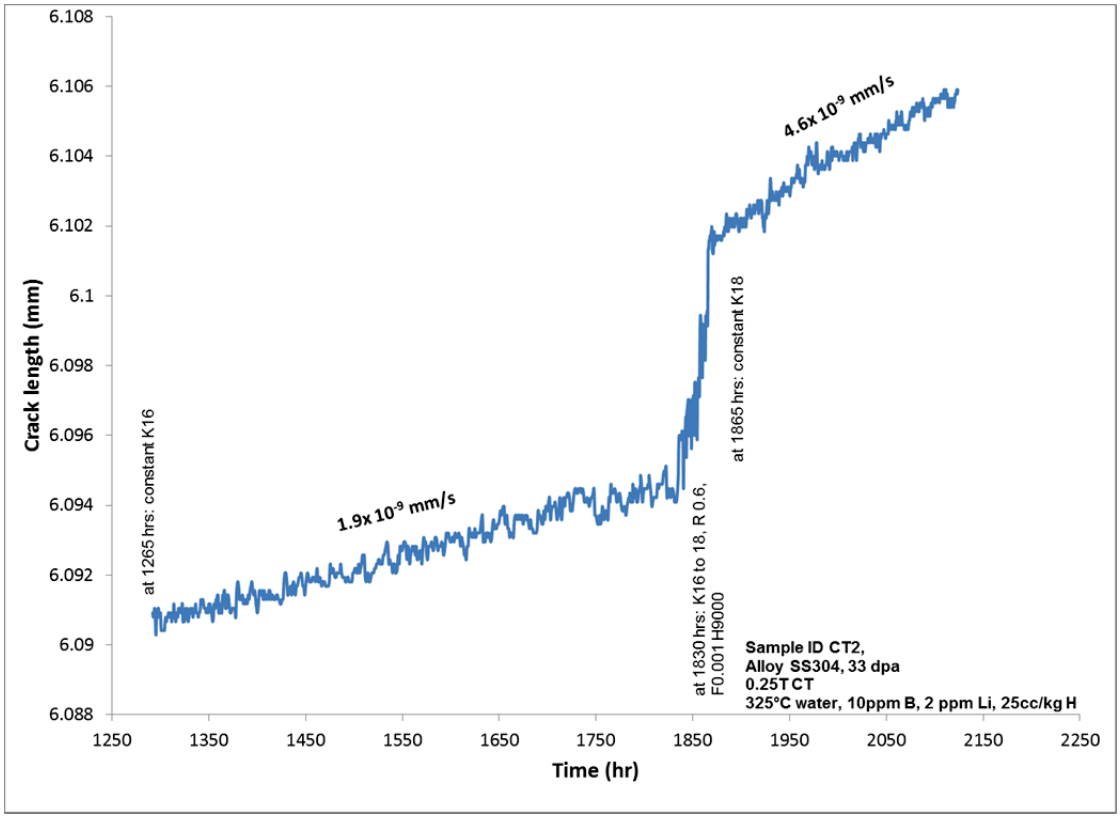

Figure 16. Effect of K applied on crack growth rate under constant K loading.

Table 1. CGR measured for each loading condition.

Steps	Planned Starting a/W	Hours	K_{max}	R	Frequency, Hz	Hold Time, Seconds	CGR (mm/s)
1	0.400	501	14	0.3	0.5	0	
2	0.430	529.9	15	0.4	0.5	0	1.66e-5
3	0.440	531.99	16	0.6	0.2	0	4.8e-6
4	0.450	539	16	0.6	0.05	0	1.63e-6
5	0.460	560.7	16	0.6	0.01	9,000	5.26e-7
6	0.470	628.9	16	0.6	0.001	9,000	9.96e-8
		Program interruption at a/w = 0.47038; specimen was unloaded to 200 lb Program restarted for a/w = 0.470000, K16, R0.6, F0.001, H9000					
7	0.470	0	16	0.6	0.001	9,000	1.36e-8
8	0.47105	120	16	0.6	0.01	0	6.25e-7
9	0.47508	144	16		0.001	9,000	2.6e-8
10	0.47540	169	16	0.6	0.01	9,000	1.14e-8
11	0.47549	190	16	0.6	0.01	0	5.41e-7
12	0.47806	208	16	0.6	0.01	9,000	1.18e-8
13	0.47920	501	16	0.6	0.001	9,000	1.27e-8
14	0.47958	605	16	1			1.91e-9
15	0.47973	1,600	16 to 18	0.6	0.001	9,000	
16			18	1			4.6e-9

7. REFERENCES

Bond, G. M et al., 1999,"Void swelling of annealed 304 stainless steel at ~370-385°C and PWR-relevant displacement rates," *9th International Conference on Environmental Degradation of Materials in Nuclear Power Systems – Water Reactors*, pp. 1045–1050.

Garner, F. A. and B. J. Makenas, 2006, "Recent experimental results on neutron-induced void swelling of AISI 304 stainless steel concerning its interactive dependence on temperature and displacement rate," *Fontevraud-6 Symposium on Contribution of Materials Investigations to Improve the Safety and Performance of LWRs*, Fontevraud, France, September 18 through 22, 2006, pp. 625–636.

Garner, F. A., J. E. Flinn, M. M. Hall, and B. J. Makenas, 2007, "Recent insights on neutron-induced void swelling and irradiation creep of AISI 304 stainless steel," *Proceedings of 13th International Conference on Environmental Degradation of Materials in Nuclear Power Systems*, Whistler, Canada, August 19 through 23, 2007.

Garner, F. A. et al., 2013, "Void swelling and resultant strains in thick 304 stainless steel components in response to spatial gradients in neutron flux-spectra and irradiation temperature," *Proceedings of 16th International Conference on Environmental Degradation of Materials in Nuclear Power Systems*, Asheville, North Carolina, August 11 through 15, 2013.

Garner, F. A. et al., 2014, "Measurement of void swelling in thick non-uniformly irradiated 304 stainless steel blocks using nondestructive ultrasonic techniques," *Fontevraud-8 Symposium on Contribution of Materials Investigations and Operating Experience to LWRs' Safety, Performance and Reliability* Avignon, France, September 14 through18, 2014.